

DNA methylome signatures as epigenetic biomarkers of hexanal associated with lung toxicity

Yoon Cho¹, Mi-Kyung Song², Jae-Chun Ryu^{Corresp. 1}

¹ Korea Institute of Science and Technology, Seoul, Republic of Korea

² Korea Institute of Toxicology, Jeongeup, Republic of Korea

Corresponding Author: Jae-Chun Ryu
Email address: yooncho@kist.re.kr

Background. Numerous studies have investigated the relationship of environmental exposure, epigenetic effects, and human diseases. These linkages may contribute to the potential toxicity mechanisms of environmental chemicals. Here, we investigated the epigenetic pulmonary response of hexanal, a major indoor irritant, following inhalation exposure in F-344 rats. **Methods.** Based on DNA methylation profiling in gene promoter regions, we identified hexanal-characterized methylated sites and target genes using an unpaired t-test with a fold-change cutoff of ≥ 3.0 and a p-value < 0.05 . We also conducted an integrated analysis of DNA methylation and mRNA expression data to identify core anti-correlated target genes of hexanal exposure. To further investigate the potential key biological processes and pathways of core DNA methylated target genes, Gene Ontology and Kyoto Encyclopedia of Genes and Genomes pathway enrichment analysis were performed. **Results.** 36 dose-dependent methylated genes and anti-correlated target genes of DNA methylation and mRNA in lung tissue of hexanal exposed F-344 rats were identified. These genes were involved in diverse biological processes such as neuroactive ligand-receptor interaction, protein kinase cascade, and intracellular signaling cascade associated with pulmonary toxicity. These results suggest that novel DNA methylation-based epigenetic biomarkers of exposure to hexanal and elucidate the potential pulmonary toxicological mechanisms of action of hexanal.

1 DNA Methylome Signatures as Epigenetic Biomarkers 2 of Hexanal Associated with Lung Toxicity

3

4 Yoon Cho¹, Mi-Kyung Song², Jae-Chun Ryu¹

5

6 ¹ Korea Institute of Science and Technology, Seoul, Republic of Korea7 ² Korea Institute of Toxicology, Jeongeup, Republic of Korea

8

9 Corresponding Author:

10 Jae-Chun Ryu¹

11 5 Hwarang-ro 14-gil, Seongbuk-gu, Seoul, 02792, Korea

12 Email address: ryujc@kist.re.kr

13

14 Abstract

15 Background.

16 Numerous studies have investigated the relationship of environmental exposure, epigenetic
17 effects, and human diseases. These linkages may contribute to the potential toxicity mechanisms
18 of environmental chemicals. Here, we investigated the epigenetic pulmonary response of
19 hexanal, a major indoor irritant, following inhalation exposure in F-344 rats.

20 Methods.

21 Based on DNA methylation profiling in gene promoter regions, we identified hexanal-
22 characterized methylated sites and target genes using an unpaired t-test with a fold-change cutoff
23 of ≥ 3.0 and a p-value < 0.05 . We also conducted an integrated analysis of DNA methylation
24 and mRNA expression data to identify core anti-correlated target genes of hexanal exposure. To
25 further investigate the potential key biological processes and pathways of core DNA methylated
26 target genes, Gene Ontology and Kyoto Encyclopedia of Genes and Genomes pathway
27 enrichment analysis were performed.

28 Results.

29 36 dose-dependent methylated genes and anti-correlated target genes of DNA methylation and
30 mRNA in lung tissue of hexanal exposed F-344 rats were identified. These genes were involved
31 in diverse biological processes such as neuroactive ligand-receptor interaction, protein kinase
32 cascade, and intracellular signaling cascade associated with pulmonary toxicity.

33 These results suggest that novel DNA methylation-based epigenetic biomarkers of exposure to
34 hexanal and elucidate the potential pulmonary toxicological mechanisms of action of hexanal.

35

36

37

38

39

40 Introduction

41 The role of epigenetics has been expanded to the field of environmental toxicology to include
42 exposure to chemical agents and pathogenesis of diseases (Watson & Goodman, 2002; Szyf,
43 2011). It is defined as environmental epigenetics (Ho et al., 2012) and provides important
44 insights into the linkage between environmental exposure and human health based on
45 toxicogenomic concepts (Burriss & Baccarelli, 2014; Reamon-Buettner et al., 2008).

46 The implication of environmental epigenetics in toxicogenomics has been demonstrated in
47 numerous studies. It may provide the cellular and molecular signatures affected by exposure to
48 environmental factors and contribute to understanding epigenetic toxicological mechanisms
49 (Baccarelli, 2009). This approach is used for developing exposure biomarkers for detecting the
50 response at low doses, early effects and elucidating the underlying modes of action for
51 environmental disease (McHale et al., 2010). Therefore, it has been considered an effective
52 strategy for toxicological risk assessment of environmental chemicals.

53 Exposure to a variety of environmental factors induces epigenetic alterations which emerge as
54 key factors of numerous important cellular processes including regulation in gene expression.

55 Also, aberrant epigenetic patterns are critical for the development of diseases and cancer
56 progression (Zoghbi & Beaudet, 2016; Kagohara et al., 2018; Koh & Hwang, 2019).

57 Furthermore, recent studies have highlighted the importance of epigenetic biomarkers such as
58 miRNA and DNA methylation-based biomarkers. Epigenetic biomarkers are emerging as
59 screening tools for exposure and risk assessments of environmental chemicals (Ray et al., 2014).
60 However, the use of epigenetic changes as a predictive exposure biomarker for exposure to
61 environmental toxicants remains unclear. Here, we aimed to identify the epigenetic biomarkers
62 of hexanal (hexaldehyde) for exposure and risk assessment based on the DNA methylome
63 signature.

64 Hexanal is one among the aldehydes which are classified as microbial volatile organic
65 compounds (mVOCs). mVOCs are emitted during metabolism in micro-organisms, including
66 fungi and bacteria. It is known that mVOCs are highly abundant in the indoor environment
67 (Korpi et al., 2009). Previous studies demonstrated that exposure to mVOCs may induce diverse
68 adverse health effects such as irritation of the respiratory tract and eyes and inflammatory
69 responses (Korpi et al., 2009; Thorn & Greenman, 2012). Of the more than 1,000 compounds of
70 mVOCs, aldehydes are a predominant group (Garcia-Alcega et al., 2018). However, the
71 toxicological data of mVOCs using omics technologies is still not well understood. We
72 previously investigated the toxicogenomic response of hexanal, an important indoor air pollutant,
73 using an in vitro system (Cho et al., 2014; 2015). In this study, we aimed to investigate the
74 epigenetic response based on DNA methylation of hexanal exposure using the in vivo model
75 system.

76 To clarify the DNA methylation networks by exposure to hexanal associated with lung toxicity,
77 we analyzed the DNA methylation profiling of lung tissues of F-344 rats following inhalation
78 exposure to hexanal. In the three hexanal inhalation exposure groups (600, 1,000, and 1,500

79 ppm), the expression of 73 methylated genes was altered and 36 dose-dependent methylated
80 genes were also identified using a 3.0-fold change cut-off and p-value < 0.05.
81 To further investigate the effect of hexanal exposure on DNA methylation and gene expression
82 profiles, we conducted an integrated analysis of the DNA methylation and mRNA expression
83 profiles. Core anti-correlated genes which are involved in key biological processes associated
84 with pulmonary toxicity were identified. These results provide that a novel epigenetic biomarker
85 of exposure to hexanal and potential important quantitative biomarkers for risk assessments. This
86 approach of DNA methylation-environmental factors may also reveals new mechanistic insights
87 on the epigenetic actions of pulmonary toxicity.

88

89 **Materials & Methods**

90 **Vertebrate Animal Study**

91 **Test animal**

92 Forty male and female Fischer 344 rats of both sexes (10 rats/group), 7 weeks of age, were
93 purchased from ORIENT BIO INC. (Seongnam, Korea). Prior to the experiment, animals were
94 housed in stainless-steel cages (255W×3465L×3200H mm) and acclimated for 5 days.
95 Purification and quarantine periods were 3 or less, and during pretest and exposure periods, 2 or
96 less were kept in stainless-steel cages. During the acclimation period, all animals are observed
97 once a day to see clinical symptoms caused by the disease. Animals with diseases or
98 abnormalities observed on physical examination are euthanized through CO₂ inhalation. Animal
99 rooms had a 12-h light/dark cycle and controlled temperature (22±3 °C) and humidity (30-70%).
100 All animals were given a sterilized commercial pellet diet (PMI Nutrition International, USA)
101 and sterilized water. All experimental procedures were approved by the Institutional Animal
102 Care and Use Committee (IACUC) of Korea Institute of Toxicology (IACUC No. 1311-0301).

103

104 **Clinical, biochemical and histopathological examinations**

105 Test animals were subjected to examine every day for any clinical, blood biochemical and
106 histopathological symptoms and mortality. Total body weight was measured twice a week during
107 the 4 weeks exposure period. Test animals surviving to the end of the exposure period received
108 completed necropsy. Test animals were euthanized using isoflurane anesthesia. For autopsy
109 animals, gross autopsy findings were observed before organ weight measurement. Whole blood
110 (WB) was rapidly collected for blood biochemical analysis from the abdominal aorta under
111 isoflurane. Serum was obtained from WB by centrifuging at 3,000 x rpm for 10 minutes at room
112 temperature and analyzed for AST(Aspartate aminotransferase), ALT(Alanine
113 aminotransferase), ALP (Alkaline phosphatase), CK((Creatine phosphokinase), GLU (Glucose),
114 TP (Total protein), ALB (Albumin), GLO (Globulin), A/G (Albumin/globulin ratio), BUN
115 (Blood urea nitrogen), CREA (Creatinine), TG (Triglyceride), PL (Phospholipid), TCHO (Total
116 cholesterol), TBIL (Total bilirubin), GGT (Gamma glutamyl transferase), Ca(Calcium),
117 IP(Inorganic phosphorus), Cl(Chloride), Na(Sodium) and K(Potassium) using an autochemical
118 analyzer, Toshiba 120FR NEO(Toshiba Co., Japan). The lung tissues were collected from all

119 animals and preserved in 10% neutral buffered formalin and embedded with paraffin wax.
120 Tissues were stained with hematoxylin and eosin (H&E) (Cho et al., 2016; 2017).

121

122 **Exposure design**

123 All animal experiments were carried in accordance with relevant guidelines and regulations.
124 Exposure experiments were designed following the OECD guideline for the testing of chemicals
125 No. 412 “Subacute Inhalation Toxicity” (OECD, 2009), considering animal welfare. Hexanal
126 vapor was generated with a bubbling generator and animals were exposed to it inside a flow-past
127 nose-only inhalation chamber. Hexanal exposure concentrations were at target levels of 600,
128 1,000, and 1,500 ppm, and the control group was exposed to filtered clean air. Grouped animals
129 had a pre-exposure period of about 2 days before exposure began. During the pre-exposure
130 period, holder adaptation training was performed in accordance with the standard operation
131 procedure to reduce stress caused by non-inhalational exposure. Residual animals excluded from
132 the test were euthanized with CO₂. The animals (10 rats per group) were exposed to hexanal for
133 4 weeks (4 h/day, 5 days/week) in the nose-only inhalation chamber. Using a GC-FID
134 (SHIMADZU, Japan), exposure concentration of hexanal vapor was measured thrice daily. We
135 also monitored the environment in the inhalation chamber such as chamber flow rate,
136 temperature (°C), relative humidity (%), chamber pressure (-Pa) and oxygen concentration (%)
137 more than 4 times during the exposure period (Cho et al., 2016; 2017).

138

139 **DNA preparation**

140 Genomic DNA was isolated from the homogenized lung tissue of rats, and only the supernatant
141 was used for extraction. DNA samples of 6 rats from each group (control, low-dose, middle-
142 dose, and high-dose group; a total of 24 DNA samples) were used for the microarray analysis for
143 all 40 rats used in the study. Using Qiagen's QIAamp DNA Mini kit (QIAGEN, Hilden,
144 Germany), genomic DNA was extracted as described in our previous study (Cho et al., 2018).
145 The genomic DNA purity and concentration were measured using ND-1000 spectrophotometer
146 (NanoDrop Technologies, Wilmington, DE) and electrophoresis conducted in a 1.5% agarose gel
147 in 1 X TAE buffer (4.8 g of Tris, 1.14 mL of acetic acid, 2 mL of 0.5 M EDTA at pH 8.0, and
148 ethidium bromide) at a constant 100 V for 15 min.

149

150 **Fragmentation of DNA**

151 To extract only methylated DNA, the genomic DNA size should be about 200 bp to 1,000 bp.
152 Therefore, genomic DNA was fragmented into 200 bp to 1,000 bp sections using a Sonic
153 Dismembrator 550 (Fisher Scientific, USA) with 3 cycles comprising 4 cycles of 20 sec 'ON' and
154 1 cycle of 20 sec 'OFF'. To determine the size of the fragmented DNA, agarose gel
155 electrophoresis and ethidium bromide staining were performed using DNA size markers of 500-
156 10,000 base pairs in size.

157

158 **Methylated DNA immunoprecipitation (MeDIP)**

159 As described in our previous study (Cho et al., 2018), MeDIP was performed with MethylMiner
160 Methylated DNA Enrichment Kit (Invitrogen, Carlsbad, CA, USA) according to the
161 manufacturer's instructions. Fragmented DNA 1 µg and untreated control DNA (Input) 3 µg were
162 used for quality and labelling procedures. Briefly, Dynabeads M-280 Streptavidin 10 µl was
163 combined with 7 µl of MBD (methyl-CpG binding domain)-Biotin Protein. The MBD-magnetic
164 bead conjugates were washed thrice and resuspended in 1 volume of 1X bind/wash buffer. The
165 capture reaction was conducted by adding of 1 µg sonicated DNA to the MBD magnetic beads
166 on a rotating mixer for 1 h at room temperature. Next, the beads were washed three times with 1
167 X bind/wash buffer. The methylated DNA was eluted as a single fraction with a high-salt elution
168 buffer (2,000 mM NaCl). Consequently, each fraction was concentrated by ethanol precipitation
169 using 1 µL glycogen (20 µg/µL), 1/10th volume of 3 M sodium acetate (pH 5.2), and two
170 volumes of 100% ethanol, and then resuspended in 60 µL of DNase-free water. The eluted
171 methylated DNA immunoprecipitation samples were stored at -20 °C until further use. This
172 experiment protocol was referred from our previous research in Cho et al. (2018).

173

174 **Epigenome-wide DNA methylation**

175 First, whole genome amplification kit (GenomePlex Complete Whole Genome Amplification
176 Kit, SIGMA-ALDRICH, USA) was used to amplify DNA and methylated immunoprecipitation
177 (IP) samples according to the manufacturer's instructions. The amplified samples were purified
178 using the QIAQuick PCR clean-up kit (QIAGEN, Hilden, Germany). The amplified DNA and 4
179 µg of the methylated IP sample were labeled using the Bioprime labeling kit from Invitrogen
180 according to the manufacturer's instructions. The IP sample was labeled with Cy5-dUTP and the
181 input DNA sample was labeled with Cy3-dUTP and 50 µl of master mix(dNTPs-dATP, dGTP,
182 dCTP; 120 µM, dTTP; 60 µM, Cy5-dUTP or Cy3-dUTP; 60 µM). After labeling the sample, the
183 concentration was measured using an ND-1000 spectrometer (NanoDrop Technologies, Inc.,
184 Wilmington, DE).

185 Second, After checking labeling efficiency, each 2.5ug to 5ug of cyanine 3-labeled and cyanine
186 5-labeled DNA target were mixed and then resuspended with 2X hybridization buffer, Cot-1
187 DNA, and Agilent 10X blocking agent, and de-ionized formamide. Before hybridization to the
188 array, the 260ul hybridization mixtures were denatured at 95 °C for 3min and incubated at 37 °C
189 for 30min. The hybridization mixtures were centrifuged at 17,900 xg for 1min and directly
190 pipetted onto the Customized Rat Methylation Microarray (400K). The arrays hybridized at
191 65°C for 40 h using Agilent Hybridization oven (Agilent Technology, USA). The hybridized
192 microarrays were washed as the manufacturer's washing protocol (Agilent Technology, USA).
193 Third, after washing, hybridization images on the slides were scanned using the Agilent DNA
194 microarray scanner (Agilent Technologies, USA) and signals were extracted from each probe
195 using Agilent Feature Extraction software (v10.7.3.1). All data were normalized using Agilent's
196 Workbench software v7.0 according to the manufacturer's instructions (Agilent Technologies,
197 USA). The background-corrected intensity data were normalized with blank subtraction followed
198 by intra-array LOWESS normalization. The peak detection was performed with Pre-defined Peak

199 Shape detection v2.0 with a p-value < 0.01 for non-parametric test and a peak-score > 5 for
200 EVD-based score. The data were normalized by dividing the average of the signal intensity of
201 the exposed group by the normalized average of the control group. The differentially methylated
202 probes were selected using the 3.0-fold change cutoff and p-value < 0.05 . For reference, the
203 intensity dependent normalization is a technique that is used to eliminate dye-related artifacts in
204 two-color experiments that cause the cy5/cy3 ratio to be affected by the total intensity of the
205 spot. This normalization process attempts to correct for artifacts caused by non-linear rates of
206 dye incorporation as well as inconsistencies in the relative fluorescence intensity between some
207 red and green dyes.

208

209 **Integrating DNA methylation and gene expression**

210 To identify the anti-correlated methylated genes, we conducted a comparative analysis of DNA
211 methylation and mRNA expression patterns using GeneSpring GX. mRNA profiles from the
212 hexanal-exposed rats were obtained from our previous study (Cho et al., 2017). We used
213 Pearson's correlation analysis, the most appropriate statistical coefficient for a small number of
214 measures, to estimate the degree of anti-correlation (e.g., hyper methylation vs. down-regulated c
215 mRNA expression or vice versa) between any putative pairs of DNA methylation and mRNA.
216 The raw data are available from the NCBI GEO under accession number GSE60118. We
217 considered the methylated genes with methylation differences of at least 3.0-fold and mRNA
218 expression differences of at least 1.5-fold on p-value < 0.05 .

219

220 **DAVID functional enrichment analysis**

221 Using the DAVID functional annotation bioinformatics tool, we performed GO enrichment
222 analyses to understand biological functions associated with hexanal exposure. It was used to
223 determine significant biological pathways for anti-correlated target genes between DNA
224 methylation and mRNA expression associated with hexanal exposure. Fisher's exact test was
225 used to detect significant enrichment of pathways, and the resulting p-value were adjusted using
226 the Benjamini-Hochberg algorithm.

227

228 **Statistical analysis**

229 In all cases, the differences between the control and exposure group were evaluated using the
230 unpaired t-test. The p-value criterion was set at p-value < 0.05 as the level of statistical
231 significance.

232

233 **Animal Ethics**

234 The experiment protocol was authorized by the Institutional Animal Care and Use Committee of
235 Korea Institute of Toxicology (IACUC No. 1311-0301).

236

237 **Results**

238 **Monitoring of inhalation exposure concentration, environmental conditions, and**
239 **histopathologic alterations**

240 As mentioned in our previous studies (Cho et al., 2016; 2017), inhalation hexanal exposure
241 concentrations were monitored in rats using online gas chromatography (GC) every 10 min
242 during the exposure period. SPF (Specific-pathogen-free) Fischer-344 derived (CRL:CD) rats of
243 both sexes were used at the age of 7 weeks (n=10/group). The average exposure concentrations
244 were 646.03 (\pm 80.06; low-dose), 999.06 (\pm 162.08; middle-dose), and 1,525.31 (\pm 199.02;
245 high- dose) ppm. The conditions of the inhalation chamber such as temperature, relative
246 humidity, chamber pressure, and oxygen concentration were also measured (Cho et al., 2016).
247 Compared with the control group, no significant body weight, organ weight and histopathologic
248 alterations were observed after 4 weeks of hexanal exposure (Cho et al., 2017). In middle-dose
249 group, increased total bilirubin compared to control group in the male rats and decreased total
250 protein, albumin and triglyceride in the female rats were identified. These results showed no
251 significant dose-dependent changes related to hexanal exposure (Cho et al., 2017). Therefore, to
252 predict the potential adverse health effects of hexanal exposure we aimed to identify the hexanal-
253 associated genetic and epigenetic alterations using microarray-based mRNA and DNA
254 methylation to address the molecular basis of hexanal exposure relevant to respiratory system.

255

256 **DNA methylation pattern after hexanal exposure**

257 Aberrant DNA methylation has been linked to the abnormalities or disorders that induced by
258 environmental stressors including environmental chemicals (Kubota, 2016). Therefore, the
259 framework of epigenome for environmental risk assessment has been rapidly developed. First,
260 we extracted from rats exposed to hexanal of three concentrations (Low dose, 600 ppm; Middle
261 dose, 1,000 ppm; High dose, 1,500 ppm), and then genomic DNA using sonication to extract
262 only methylated DNA using immunoprecipitation. The cleaved methylated DNA was confirmed
263 using gel electrophoresis, and as a result, it was confirmed that the DNA of all groups was
264 sheared to about 150 bp to 500 bp, so that the optimal DNA for immunoprecipitation was
265 secured (Supplementary Fig.1). After methylated DNA was extracted from aldehyde-exposed rat
266 lung tissues through methylated DNA immunoprecipitation, the concentration was measured and
267 the quantitative analysis of methylated DNA was performed through gel electrophoresis. As a
268 result, it was confirmed that the concentration and state of methylated DNA are suitable for DNA
269 methylation microarray (Supplementary Fig.2). In the current study, using a custom-designed
270 Agilent 400K CpG methylation microarray, we investigated DNA methylation profiles in CpG
271 islands gene promoter sequences of hexanal-exposed lung tissues of F344 rats and compared
272 with those from rats exposed to clean filtered air (control group) (n=6/group). For reference, the
273 DNA Methylation Microarray are designed to interrogate known CpG islands and related sites. It
274 is designed for analysis of methylated DNA derived from affinity-based isolation methods
275 including methylated DNA immunoprecipitation (MeDIP). We analyzed methylation patterns for
276 approximately 389,347 probes on the arrays. Compared with the control group, all three hexanal-
277 exposed groups showed distinctly different methylation patterns (Fig.1). The data is the averaged

278 signal that is acquired from normalizing the signal intensity by dividing the average of the signal
279 intensity of the control group. In the low dose exposure group, 661 methylated sites and 571
280 differentially methylated genes (hyper-methylated: 464, hypo-methylated: 107) were identified.
281 In the middle dose exposure group, 4,181 methylated sites and 3,268 differentially methylated
282 genes (hyper-methylated: 2,513, hypo-methylated: 755) were identified, and 11,744 methylated
283 sites and 7,477 differentially methylated genes (hyper-methylated: 4,851, hypo-methylated:
284 2,662) were identified in the high dose exposure group. In all groups change was noted at ≥ 3.0 -
285 fold change, p -value < 0.05 . Overall, the methylation sites increased as the exposure
286 concentration increased. (Table 1).

287 Among these differentially methylated sites and genes, 79 sites and 73 genes (hyper-methylated:
288 69, hypo-methylated: 4) showed commonly methylated expression patterns in the three hexanal
289 exposure groups (Fig. 2, Table 2). Furthermore, we identified 36 dose-dependent methylated
290 genes (34 hyper-methylated and 2 hypo-methylated) in the common methylated genes of three
291 hexanal exposure group using line-plot analysis (Fig. 3.A, Table 3). The dose-dependent genes
292 are illustrated as a heatmap (Fig. 3.B). These dose-response relationships have the potential to
293 serve as quantitative epigenetic biomarkers of hexanal exposure. Raw data are available online at
294 Gene Expression Omnibus (GEO accession number GSE129313).

295

296 **Gene expression profiles induced by hexanal exposure**

297 To investigate the gene expression signatures response to hexanal inhalation exposure, we
298 previously investigated the gene expression profiling of lung tissues of hexanal-exposed F344
299 rats using the Rat Oligo Microarray (44 K). The raw data are available at GEO/NCBI GSE
300 60118. The gene expression profiles were analyzed by comparing them to the control group
301 using 1.5-fold change and unpaired t-test p value < 0.05 as statistical significance (Table 4). In
302 the previous study, we identified hexanal specific genes that were involved in diverse biological
303 processes including apoptosis, cell proliferation, and mitogen-activated protein kinase (MAPK)
304 cascade. These genes were also associated with disease such as respiratory and nervous system
305 diseases (Cho et al., 2017). It suggests that hexanal exposure may have potential adverse health
306 effects on humans. Therefore, we aimed to analyze DNA methylation signatures in hexanal-
307 exposed F344 rats to understand the epigenetic effects of hexanal exposure.

308

309 **Comparative analysis of DNA methylation and mRNA expression profiles**

310 DNA methylation was involved in transcriptional regulation and gene activity. Promoter hyper-
311 methylation can leads to silencing of gene expression, whereas hypo-methylation can leads to
312 gene activation. The investigation of the implication of DNA methylation in the regulation of
313 gene expression and identification of key genes that regulated by both DNA methylation and
314 gene expression using integrative analysis is important. Therefore, we conducted an integrated
315 analysis of DNA methylation (Table 1.) and mRNA expression data (Table 4.). As shown in
316 Table 5, we identified the hyper-methylated vs. down-regulated genes and hypo-methylated vs.

317 up-regulated genes in the hexanal exposure groups. These results suggest potential core DNA
318 methylation-based epigenetic biomarkers for exposure/risk assessment of hexanal.

319

320 **Gene Ontology (GO) analysis of putative DNA methylation biomarkers of hexanal**

321 We next investigated the relevant molecular and cellular processes controlled by hexanal
322 exposure-specific inversely correlated target genes based on GO biological processes terms using
323 the DAVID bioinformatics tool (Table 6). The key GO terms were related to the lactation (GO:
324 0007595), skeletal muscle cell differentiation (GO:0035914), Positive regulation of synapse
325 assembly (GO:0051965), sodium ion transport (GO:0006814), and regulation of tumor necrosis
326 factor production (GO:0032680). These results indicated that putative epigenetic biomarkers of
327 hexanal are involved in skeletal muscle cell differentiation, synapse assembly, and TNF
328 production. Further studies are necessary to determine hexanal-induced toxicological
329 mechanisms based on functional enrichment analysis.

330

331 **Discussion**

332 Traditional toxicity testing depends on animal testing to investigate the risk of chemicals to
333 human health. It requires several animals, high investment, and a significant amount of time.
334 Additionally, it should consider ethical treatment of animals and their welfare. Therefore, this
335 approach is insufficient to handle risk assessments of the large number of chemicals in the
336 environment (Chen et al., 2012; North & Vulpe, 2010), and novel strategies for toxicological risk
337 assessment of environmental chemicals are necessary.

338 In response to these challenges, the field of toxicogenomics has been established and developed
339 rapidly for risk assessments. Toxicogenomics includes high-throughput technologies such as
340 transcriptomics, proteomics, and metabolomics for predictive toxicology and risk assessment
341 (Hamadeh et al., 2002). Currently, an integrated framework for multi-omics has been proposed.
342 It provides insight into the mode of action of environmental toxicants and helps in understanding
343 the underlying mechanisms of toxicants and adverse outcome pathways (AOPs) (Williams et al.,
344 2014). In contrast to traditional toxicity methods, it is possible to also identify multiple-response
345 and endpoints using toxicogenomics.

346 Toxicogenomics study has developed rapidly with microarray and next generation sequencing
347 technologies. The microarray technology was proposed in the 1990s (Chen et al., 2012). It is a
348 powerful tool for evaluating the effect of environmental chemicals on human health, providing
349 valuable genomic information for identifying biomarkers related to occupational exposure and
350 disease prognosis (Jung et al., 2017; Gwinn & Weston, 2008; Kim et al., 2016). It allows
351 simultaneous screening of the expression levels of thousands of genes exposed to environmental
352 toxicants based on omics tools. Therefore, toxicogenomics has been considered as a new
353 toxicology paradigm for risk assessment and prediction of exposure and risk of environmental
354 chemicals.

355 One of the epigenome studies demonstrated that DNA methylation has an important role in the
356 regulation of gene expression and epigenetic phenotype variation (Hong et al., 2018) leading to

357 insights into the development of diseases associated with environmental risk assessment (Ray et
358 al., 2014; Conerly & Grady; 2010). Generally, the expression patterns of DNA methylation are
359 altered by environmental factors, including environmental chemicals, air pollution, and
360 nonchemical stressors. Moreover, it has been linked to levels of health, disease susceptibility,
361 and disease development (Martin & Fry; 2018). Therefore, epigenetic modifications can be novel
362 exposure biomarkers of the diseases related to environmental factors.

363 To investigate the epigenetics actions of hexanal associated with lung toxicity, we aimed to
364 identify epigenetic biomarkers based on DNA methylation. As major component of indoor air
365 pollutants, we previously analyzed the transcriptome profiles of hexanal using in vitro and in
366 vivo models (Cho et al., 2014; 2017). And we also analyzed the methylation profiles of seven
367 aldehydes (propanal, butanal, pentanal, hexanal, heptanal, octanal, and nonanal) exposed human
368 lung epithelial cell, A549, to investigate the aldehydes exposure and epigenetic alterations based
369 on DNA methylation (Cho et al., 2018). Here, we proposed three steps of DNA methylome
370 analysis of hexanal exposure using the in vivo model. First, we identified the differentially
371 methylated genes of hexanal exposure showing a 3.0-fold-change ($p < 0.05$). Of the 389,347
372 probes on the customized rat 400K CpG methylation microarray, the methylated genes identified
373 showed significant expression changes in the three hexanal exposure groups (low dose, middle
374 dose, and high dose) compared to the control group. Among the differentially methylated genes,
375 we identified commonly methylated genes and dose-dependent methylated patterns, which
376 provided significant novel epigenetic biomarkers of hexanal exposure. These methylated genes
377 were involved in chemical stimulus associated with olfactory receptor activity (OLR1696,
378 OLR500, OLR5, OLR407, OLR1085, OLR1084, OLR1389), insulin stimulus (PLA2G1B,
379 MYO5A, USF1) and negative regulation of peptidyl-serine phosphorylation (HGF, INPP5J). The
380 follow-up studies will be necessary to address a pulmonary toxicological mechanisms associated
381 with hexanal exposure. Also, the dose-response relationship plays essential role in the field of
382 toxicology, it provides the determination of threshold for toxic effect and better understanding of
383 network for exposure-human health (Tsatsakis et al., 2018).

384 Second, we analyzed the transcriptome profiles of hexanal exposure in F344 rats to investigate
385 the hexanal-characterized genes and environmental chemical-gene interactions based on
386 toxicogenomics (Cho et al., 2017). Third, we conducted the comparative analysis of genome-
387 wide DNA methylome and transcriptome in the hexanal- exposed F344 rats. It is well known that
388 the DNA methylation is associated with gene expression. DNA hypermethylation results in gene
389 silencing and hypomethylation leads to elevated transcription (Li et al., 2017). The identification
390 of key genes that regulated by both DNA methylation and mRNA expression system via
391 integrative analysis is necessary. Therefore, we aimed to identify the novel biomarkers that anti-
392 correlated between DNA methylation and gene expression. Together, these processes can serve
393 to determine the important framework for environmental epigenetics in exposure/risk assessment
394 and it allows the identification of the critical bridging epigenetic biomarkers of hexanal. Further
395 biomarker validation and developing studies are necessary to explore the specificity, sensitivity
396 and implications of these biomarkers. And then, it is predicted that this epigenetic biomarkers

397 can be used to determine whether exposure to hexanal and to determine the cause of
398 environmental diseases.

399 *In vivo* models including rat model are essential for evaluating the toxicity of inhaled factors for
400 the risk assessment on human health. It is fundamental for understanding the mammalian system
401 including human biology at molecular level. Therefore, we used the F344 rat models to evaluate
402 the pulmonary toxicity of hexanal associated with human adverse health effects. In this study, the
403 analyzed DNA methylated genes at CpG islands were conserved in human. It has orthologs
404 between rat and human.

405 Most of aldehydes inhalation toxicity research has progressed extensively on formaldehyde and
406 acetaldehyde, which are classified as Group 1 carcinogenes by IARC (International Agency for
407 Research on Cancer). However, other aldehydes such as hexanal toxicological data are relatively
408 insufficient for risk assessment. Therefore, we aimed to investigate the inhalation toxicity of
409 hexanal using F344 rats. For reference, in this study, hexanal exposure doses (low dose, 600 ppm;
410 middle dose, 1,000 ppm; and high dose, 1,500 ppm) were selected based on the LC_{Lo} (Lowest
411 Lethal Concentration; 2,000 ppm/4hr) of hexanal using nose-only inhalation chamber. These
412 exposure dose levels that are much higher than actually exposed levels in environment. Since the
413 VOCs are typically exposed to low levels for long-term, we determined the hexanal exposure
414 doses higher than the actual exposure levels to investigate the clear implications for human
415 health.

416 Using the DAVID functional annotation bioinformatics tool, GO analysis was also performed.
417 GO enrichment analysis demonstrated that cell differentiation of skeletal muscle cells, regulation
418 of synapse assembly and regulation of TNF production are involved in major biological process
419 associated with hexanal exposure. Among them, BTG2, ZFP36 and ASIC2 were commonly
420 involved in hexanal related biological processes such as skeletal muscle cell differentiation and
421 regulation of nuclear-transcribed mRNA poly (A) tail shortening. BTG2 (BTG anti-proliferation
422 factor 2) has important roles in control of cell growth, cell differentiation, apoptosis and
423 transcriptional regulation. Moreover, it is involved in tumor progression in response to a variety
424 of stressors, steroid hormones and growth factors (Yuniati L et al., 2019). ZFP36 (Zinc finger
425 protein 36 homolog; also known as Tristetraprolin) plays role in regulation of TNF- α (Tumor
426 necrosis factor-alpha) expression which is a pro-inflammatory mediator (Zhao XK et al., 2016).
427 Since we identified that the relationship between the TNF regulation and hexanal exposure using
428 GO analysis, we considered that further research on inflammatory mechanisms via TNF
429 associated with ZFP36 expression is required. ASIC2 (Acid sensing ion channel subunit 2) is
430 expressed in several systems including peripheral and central nervous system as
431 mechanoreceptor and acid receptor (Kikuchi et al., 2008). Recent studies demonstrated that
432 ASIC2 may lead to increase the pulmonary vascular resistance and possibility of hypoxic
433 pulmonary hypertension (Detweiler et al., 2019).

434 These results reflect that hexanal exposure may affect skeletal muscle and neuronal system as
435 well as respiratory system. Further validation of key toxicological mechanisms induced by
436 hexanal exposure such as pulmonary inflammation via TNF signaling pathway is required.

437

438 Conclusions

439 Taken together, this study demonstrated the characteristic methylated profiles by hexanal
440 inhalation exposure system using DNA methylome analysis in an in vivo model. By integrating
441 DNA methylation and mRNA expression profiles, target genes were identified. These genes
442 could be valuable epigenetic biomarkers to distinguish exposure to hexanal and to determine the
443 DNA methylome responses to hexanal exposure in the environment and to predict the underlying
444 mechanisms of hexanal exposure associated with pulmonary toxicity. Further studies on these
445 methylated signatures are required to provide insights into the molecular toxicological
446 mechanisms activated by hexanal exposure.

447

448 Acknowledgements**449 Conflict of Interest**

450 The authors declare that there are no conflicts of interest.

451

452 Author Contributions

453 Yoon Cho performed the experiments, analyzed the data, and wrote the manuscript; Mi-Kyung
454 Song designed the research and performed the experiments; Jae-Chun Ryu conceived and
455 designed the research, and supervised the work.

456

457 References

- 458 Baccarelli, A., Bollati, V. Epigenetics and environmental chemicals. *Curr Opin Pediatr.* 21(2),
459 243-251 (2009).
- 460 Burris, H.H., Baccarelli, A.A. Environmental epigenetics: from novelty to scientific discipline. *J*
461 *Appl Toxicol.* 34(2), 113-116 (2014).
- 462 Chen, M., Zhang, M., Borlak, J., Tong, W. A decade of toxicogenomic research and its
463 contribution to toxicological science. *Toxicol Sci.* 130(2), 217-228 (2012).
- 464 Cho, Y., Song, M.K., Choi, H.S., Ryu, J.C. Analysis of Dose-response to Hexanal-induced Gene
465 Expression in A549 Human Alveolar Cells. *BioChip J.* 8(2), 75-82 (2014).
- 466 Cho, Y, Lim J.H., Jeong, S.C., Song, M.K., Ryu J.C. Hexanal-induced Changes in miRNA-
467 mRNA Interactions in A549 Human Alveolar Epithelial Cells. *Toxicol. Environ. Health. Sci.*
468 7(2), 143-159 (2015).
- 469 Cho, Y., Song, M.K., Jeong, S.C., Lee, K., Heo, Y., Kim, T.S., Ryu, J.C. MicroRNA response of
470 inhalation exposure to hexanal in lung tissues from Fischer 344 rats. *Environ Toxicol.* 31(12),
471 1909-1921 (2016).
- 472 Cho, Y., Lim, J.H., Song, M.K., Jeong, S.C., Lee, K., Heo, Y., Kim, T.S., Ryu, J.C.
473 Toxicogenomic analysis of the pulmonary toxic effects of hexanal in F344 rat. *Environ Toxicol.*
474 32(2), 382-396 (2017).
- 475 Cho, Y., Song, M.K., Kim, T.S., Ryu, J.C. DNA Methylome Analysis of Saturated Aliphatic
476 Aldehydes in Pulmonary Toxicity. *Sci Rep.* 8(1):10497 (2018).

477 Conerly, M., Grady, W.M. Insights into the role of DNA methylation in disease through the use
478 of mouse models. *Dis Model Mech.* 3(5-6), 290-297 (2010).

479 Detweiler ND, Herbert LM, Garcia SM, Yan S, Vigil KG, Sheak JR, Resta TC, Walker BR,
480 Jernigan NL. Loss of acid-sensing ion channel 2 enhances pulmonary vascular resistance and
481 hypoxic pulmonary hypertension. *J Appl Physiol* (1985). 127(2), 393-407 (2019).

482 Garcia-Alcega, S., Nasir, Z.A., Ferguson, R., Noël, C., Cravo-Laureau, C., Whitby, C.,
483 Dumbrell, A.J., Colbeck, I., Tyrrel, S., Coulon, F. Can chemical and molecular biomarkers help
484 discriminate between industrial, rural and urban environments? *Science of The Total*
485 *Environment.* 631-632, 1059-1069 (2018).

486 Gwinn, M.R., Weston, A. Application of oligonucleotide microarray technology to toxic
487 occupational exposures. *J Toxicol Environ Health A.* 71(5), 315-324 (2008).

488 Hamadeh, H.K., Amin, R.P., Paules, R.S., Afshari, C.A. An overview of toxicogenomics. *Curr*
489 *Issues Mol Biol.* 4(2), 45-56 (2002).

490 Ho, S.M., Johnson, A., Tarapore, P., Janakiram, V., Zhang, X., Leung, Y.K. Environmental
491 epigenetics and its implication on disease risk and health outcomes. *ILAR J.* 53(3-4), 289-305
492 (2012).

493 Hong, Y., Hong, S.-H., Oh, Y.-M., Shin, S.-H., Choi, S.S., Kim, W.J. Identification of lung
494 cancer specific differentially methylated regions using genome-wide DNA methylation study.
495 *Mol Cell Toxicol.* 14, 315-322 (2018).

496 Jung, J., Hah, K., Lee, W., Jang, W. Meta-analysis of microarray datasets for the risk assessment
497 of coplanar polychlorinated biphenyl 77 (PCB77) on human health. *Toxicol. Environ. Health.*
498 *Sci.* 9(2), 161-168 (2017).

499 Kagohara, L.T., Stein-O'Brien, G.L., Kelley, D., Flam, E., Wick, H.C., Danilova, L.V.,
500 Easwaran, H., Favorov, A.V., Qian, J., Gaykalova, D.A., Fertig, E.J. Epigenetic regulation of
501 gene expression in cancer: techniques, resources and analysis. 17(1), 49-63 (2018).

502 Kikuchi S, Ninomiya T, Kawamata T, Tatsumi H. Expression of ASIC2 in ciliated cells and
503 stereociliated cells. *Cell Tissue Res.* 333(2), 217-24 (2008).

504 Kim, S.Y., Hong, J.Y., Yu, S.Y., Kim, G.W., Ahn, J.J., Kim, Y., Son, S.W., Park, J.T., Hwang,
505 S.Y. Identification of potential biomarkers for xylene exposure by microarray analyses of gene
506 expression and methylation. *Mol. Cell. Toxicol.* 12(1), 15-20 (2016).

507 Koh, E.J., Hwang, S.Y. Multi-omics approaches for understanding environmental exposure and
508 human health. *Mol Cell Toxicol.* 15, 1-7 (2019).

509 Korpi, A., Järnberg, J., Pasanen, A.L. Microbial volatile organic compounds. *Crit Rev Toxicol.*
510 39(2), 139-193 (2009).

511 Kubota, T. Epigenetic alterations induced by environmental stress associated with metabolic and
512 neurodevelopmental disorders. *Environ Epigenet.* 2(3):dw017 (2016).

513 Li, Z., Zhuang, X., Zeng, J., Tzeng, C.M. Integrated Analysis of DNA Methylation and mRNA
514 Expression Profiles to Identify Key Genes in Severe Oligozoospermia. *Front Physiol.* 8:261
515 (2017).

516 Martin, E.M., Fry, R.C. Environmental Influences on the Epigenome: Exposure- Associated
517 DNA Methylation in Human Populations. *Annu Rev Public Health*. 39:309-333 (2018).

518 McHale, C.M., Zhang, L., Hubbard, A.E., Smith, M.T. Toxicogenomic profiling of chemically
519 exposed humans in risk assessment. *Mutat Res*. 705(3), 172-183 (2010).

520 North, M., Vulpe, C.D. Functional toxicogenomics: mechanism-centered toxicology. *Int J Mol*
521 *Sci*. 11(12), 4796-4813 (2010).

522 Szyf, M. The implications of DNA methylation for toxicology: toward toxicomethylomics, the
523 toxicology of DNA methylation. *Toxicol Sci*. 120(2): 235-255 (2011).

524 Thorn, R.M., Greenman, J. Microbial volatile compounds in health and disease conditions. *J*
525 *Breath Res*. 6(2), 024001 (2012).

526 Tsatsakis, A.M., Vassilopoulou, L., Kovatsi, L., Tsitsimpikou, C., Karamanou, M., Leon, G.,
527 Liesivuori, J., Hayes, A.W., Spandidos, D.A. The dose response principle from philosophy to
528 modern toxicology: The impact of ancient philosophy and medicine in modern toxicology
529 science. *Toxicol Rep*. 5:1107-1113 (2018).

530 Ray, P.D., Yosim, A., Fry, R.C. Incorporating epigenetic data into the risk assessment process
531 for the toxic metals arsenic, cadmium, chromium, lead, and mercury: strategies and challenges.
532 *Front Genet*. 5, 201. doi: 10.3389/fgene.2014.00201 (2014).

533 Reamon-Buettner, S.M., Mutschler, V., Borlak, J. The next innovation cycle in toxicogenomics:
534 environmental epigenetics. *Mutat Res*. 659(1-2), 158-65 (2008).

535 Watson, R.E., Goodman, J.I. Epigenetics and DNA methylation come of age in toxicology.
536 *Toxicol Sci*. 67(1), 11-16 (2002).

537 Williams, T.D., Mirbahai, L., Chipman, J.K. The toxicological application of transcriptomics and
538 epigenomics in zebrafish and other teleosts. *Brief Funct Genomics*. 13(2), 157-171 (2014).

539 Yuniati L, Scheijen B, van der Meer LT, van Leeuwen FN. Tumor suppressors BTG1 and
540 BTG2: Beyond growth control. *J Cell Physiol*. 234(5), 5379-5389 (2019).

541 Zhao XK, Che P, Cheng ML, Zhang Q, Mu M, Li H, Luo Y, Liang YD, Luo XH, Gao CQ,
542 Jackson PL, Wells JM, Zhou Y, Hu M, Cai G, Thannickal VJ, Steele C, Blalock JE, Han X,
543 Chen CY, Ding Q. Tristetraprolin Down-Regulation Contributes to Persistent TNF-Alpha
544 Expression Induced by Cigarette Smoke Extract through a Post-Transcriptional Mechanism.
545 *PLoS One*. 11(12), e0167451. doi: 10.1371/journal.pone.0167451 (2016).

546 Zoghbi, H.Y., Beaudet, A.L. Epigenetics and Human Disease. *Cold Spring Harb Perspect Biol*.
547 8(2), a019497 (2016).

548

Figure 1

Total DNA methylation expression profiles of hexanal exposed in F-344 rats (n=6/group).

Total DNA methylation expression profiles of hexanal exposed in F-344 rats (n=6/group). Two-dimensional diagram of the characteristic expression profiles of 389,247 classifier methylation probes. Rows (y-axis) represent the intensity of the DNA methylation probes and columns (x-axis) represent the different experimental conditions. Color intensity reflects differences in expression between sample DNA and reference DNA.

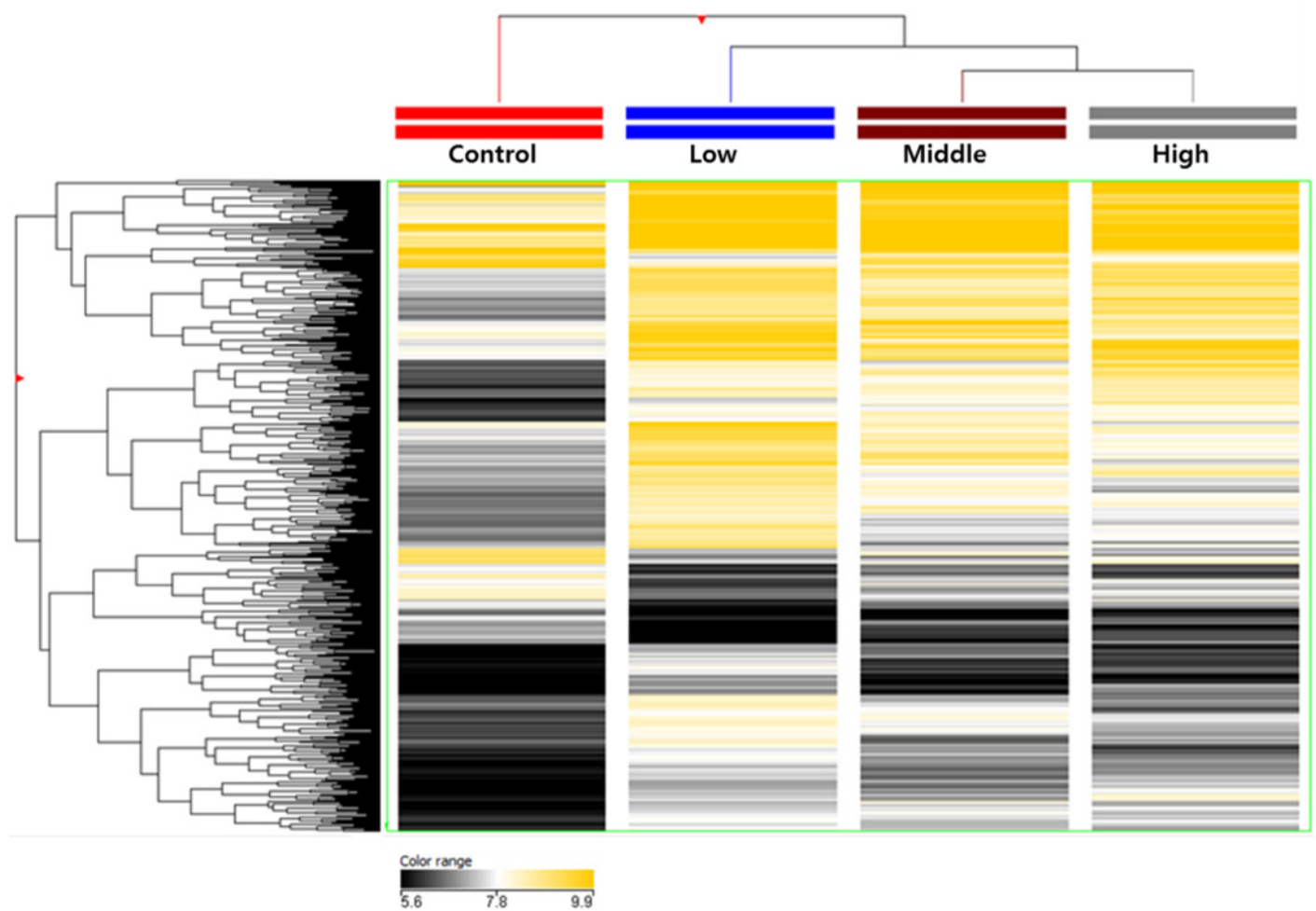


Figure 2

The Venn diagram and hierarchical clustering image of hexanal specific methylated DNA

(A) The Venn diagram and (B) hierarchical clustering image shows that 73 methylated DNA that commonly altered their expression are identified in three dose - T1(600ppm), T2(1,000ppm) and T3(1,500ppm) with a fold-change ≥ 3.0 -fold and p -value < 0.05 compared to the control group (Filtered air) (Yellow: hypermethylation; Black: hypomethylation).

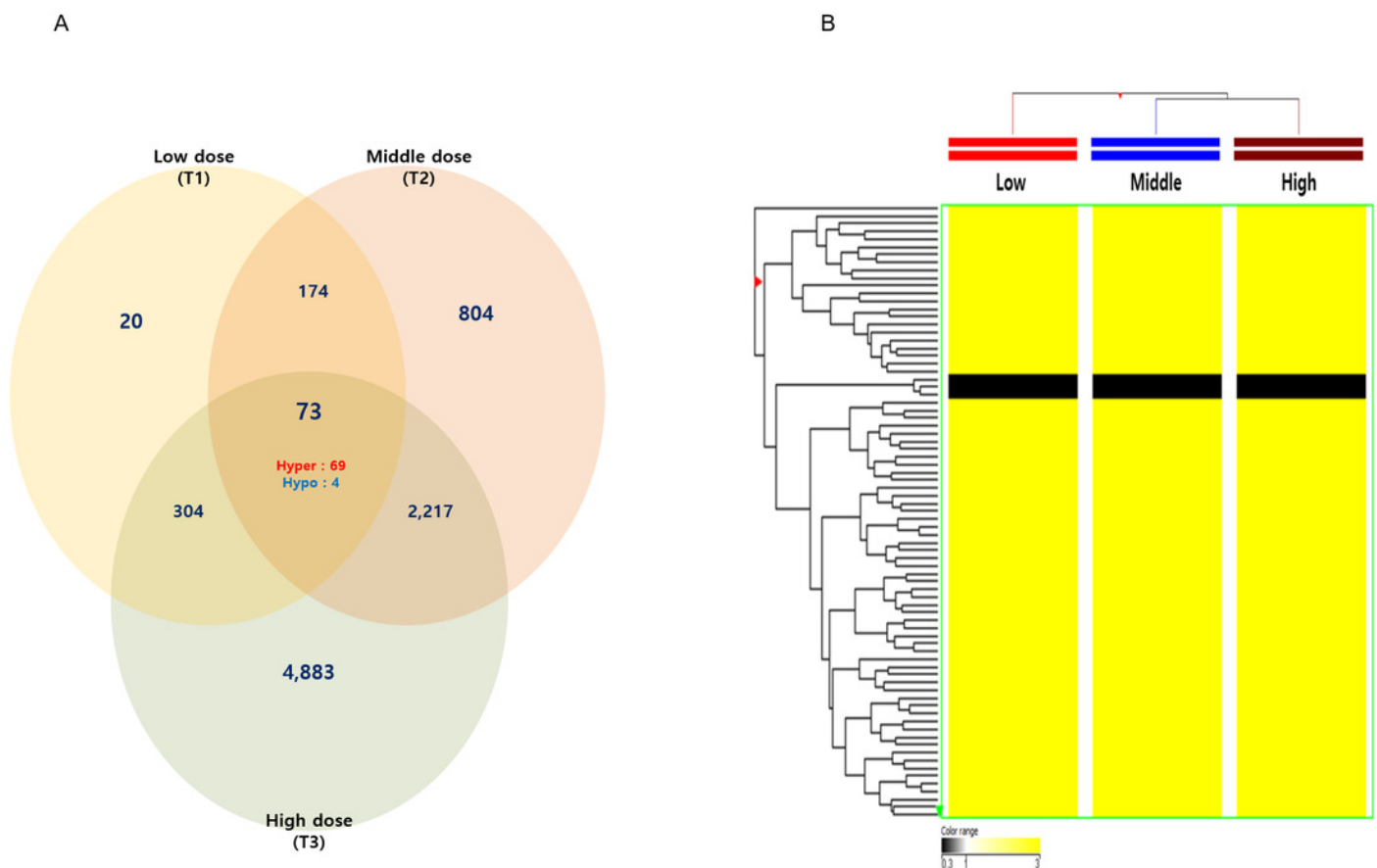


Figure 3

Line plot and heatmap of dose-dependent response of methylated genes by hexanal exposure

(A) Line plot showed dose-dependent response of methylated genes by hexanal exposure. Each line of the plot represents the normalized intensity values by the control group shown on the x-axis. The y-axis has a log₂ scale. (B) The heatmap of 36 dose-dependent methylated genes by hexanal exposure.

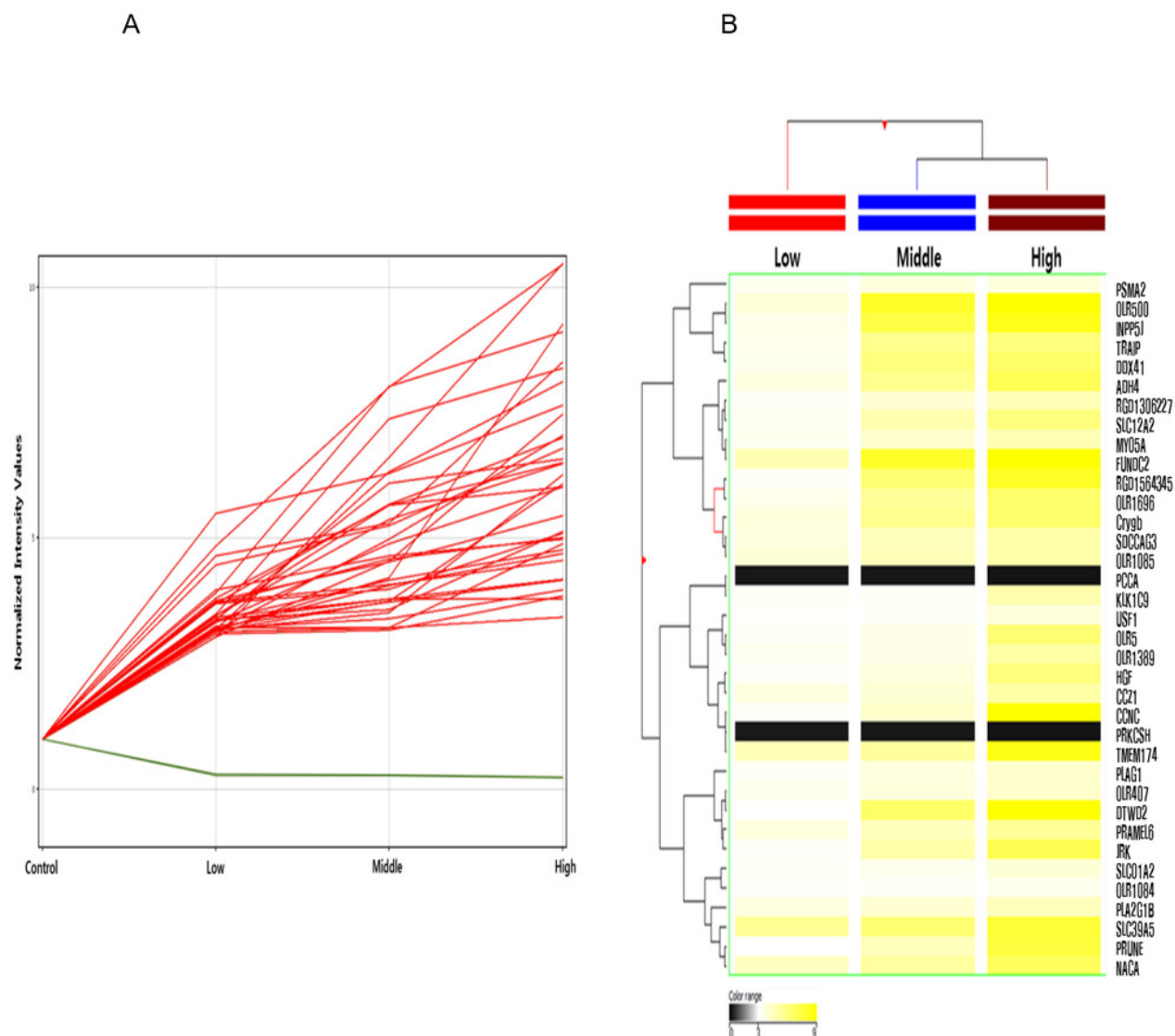


Table 1 (on next page)

The DNA methylated sites and regulated target genes in three hexanal exposure groups.

- 1 Table 1. The DNA methylated sites and regulated target genes in three hexanal exposure group.

Exposure dose	Methylated sites	Regulated target genes
Low dose (600 ppm)	661	571
Middle dose (1,000 ppm)	4,181	3,268
High dose (1,500 ppm)	11,744	7,477

2

Table 2 (on next page)

The list of 73 methylated target genes that commonly altered their expression in three hexanal exposure group.

The list of 73 methylated target genes that commonly altered their expression in three hexanal exposure group.

- 1 Table 2. The list of 73 methylated target genes that commonly altered their expression in three hexanal exposure group.

Probe ID	Annotation	Fold change			Regulation
		Low dose (T1)	Middle dose (T2)	High dose (T3)	
RP14104253	Kcng1	0.31	0.27	0.33	down
RP14316148	Pcca	0.28	0.28	0.23	down
RP14196310	Prkesh	0.30	0.29	0.24	down
RP14232470	Sstr5	0.27	0.29	0.18	down
RP14072666	Adh4	3.69	5.67	6.99	up
RP14052111	Ankrd34b	3.34	5.67	3.86	up
RP14347714	Atp9b	3.82	5.05	3.70	up
RP14104488	Bcas1	4.10	3.07	6.10	up
RP14068918	Capza1	4.21	3.73	5.01	up
RP14275323	Ccl24	3.38	3.97	3.64	up
RP14132603	Ccnc	3.17	4.21	9.26	up
RP14271990	Ccz1	3.69	3.98	5.10	up
RP14133935	Chmp5	3.55	3.30	3.65	up
RP14222274	Crygb	3.80	5.65	6.50	up
RP14271525	Cyp3a23/3a1	3.04	4.79	4.29	up
RP14329375	Ddx41	3.38	6.09	6.58	up
RP14200524	Dpagt1	3.15	3.10	4.53	up
RP14344056	Dtwd2	3.03	6.60	10.47	up
RP14214176	Eif1b	4.11	4.07	12.637	up
RP14372792	Fam228a	3.13	4.24	3.59	up
RP14266770	Fgf12	4.25	3.27	3.56	up
RP14338669	Fundc2	4.84	8.01	10.45	up
RP14253846	G6pc3	4.79	3.86	3.74	up

RP14008399	Gltscr2	3.38	4.32	4.30	up
RP14108468	Hgf	3.15	3.74	6.07	up
RP14139108	Hook1	4.25	3.50	5.47	up
RP14301839	Inpp5j	3.49	7.37	8.39	up
RP14183524	Jrk	3.15	4.97	7.04	up
RP14214724	Kif15	3.23	4.71	4.62	up
RP14016091	Klk1c9	3.21	3.21	4.89	up
RP14248629	LOC303448	3.74	5.28	4.63	up
RP14343955	LOC317165	3.44	4.13	3.41	up
RP14299892	Lyar	3.51	4.27	3.36	up
RP14208423	Mrap2	3.18	5.16	4.73	up
RP14207074	Myo5a	3.37	4.16	4.77	up
RP14169885	Naca	4.46	5.24	6.78	up
RP14301172	Nelfa	4.68	3.28	4.22	up
RP14171345	Olr1049	3.31	3.21	4.30	up
RP14175180	Olr1084	3.14	3.22	3.42	up
RP14175183	Olr1085	3.97	4.65	4.98	up
RP14199556	Olr1328	3.99	3.65	5.69	up
RP14235002	Olr1389	3.38	3.57	5.12	up
RP14307926	Olr1624	9.62	24.83	12.97	up
RP14359583	Olr1696	3.46	5.37	6.49	up
RP14359635	Olr1701	4.19	3.05	5.11	up
RP14080399	Olr407	3.43	3.79	4.18	up
RP14085578	Olr448	3.37	4.72	4.11	up
RP14006401	Olr5	3.17	3.51	6.25	up
RP14086255	Olr500	3.90	8.02	9.10	up
RP14342389	Pcdhb12	3.26	3.18	3.44	up

RP14280875	Pitpnb	3.81	5.59	4.57	up
RP14279738	Pla2g1b	3.73	4.07	4.56	up
RP14131422	Plagl	3.24	3.72	4.16	up
RP14086989	Pramel6	3.75	4.52	5.44	up
RP14066541	Prune	3.03	4.54	7.46	up
RP14335189	Psm2	3.35	3.78	3.78	up
RP14055154	RGD1306227	3.18	4.06	4.69	up
RP14108982	RGD1564345	3.18	6.32	8.11	up
RP14374247	Rhox3	3.24	4.87	3.71	up
RP14029004	rnf141	3.05	8.04	5.87	up
RP14212856	Rtp3	3.35	6.35	5.19	up
RP14076254	Sdccag3	3.69	4.58	5.01	up
RP14344660	Slc12a2	3.32	4.88	6.02	up
RP14170272	Slc39a5	5.49	6.28	7.65	up
RP14130014	Slco1a2	3.20	3.40	3.96	up
RP14165691	Slirp	3.82	4.60	4.47	up
RP14049010	Taf5	3.19	4.32	3.27	up
RP14053110	Tmem174	5.15	4.73	4.69	up
RP14211530	Traip	3.45	5.65	6.02	up
RP14096780	Trmt6	4.06	3.93	5.93	up
RP14013877	Tyrbp	3.60	4.79	3.66	up
RP14288987	Usf1	3.09	3.16	3.85	up
RP14237317	Zfp672	3.69	5.22	4.65	up

Table 3 (on next page)

The dose-dependent methylated target genes in three hexanal exposure groups.

1 Table 3. The dose-dependent methylated target genes in three hexanal exposure group.

Probe ID	Annotation	Fold change			Regulation
		Low dose (600 ppm)	Middle dose (1,000 ppm)	High dose (1,500 ppm)	
RP14196310	Prkesh	0.30	0.29	0.24	Down
RP14316148	Pcca	0.28	0.28	0.23	Down
RP14006401	Olr5	3.17	3.51	6.25	Up
RP14016091	Klk1c9	3.21	3.21	4.89	Up
RP14053108	Tmem174	4.64	5.29	8.50	Up
RP14055154	RGD1306227	3.18	4.06	4.69	Up
RP14066541	Prune	3.03	4.54	7.46	Up
RP14072666	Adh4	3.69	5.67	6.99	Up
RP14076254	Sdccag3	3.69	4.58	5.01	Up
RP14080399	Olr407	3.43	3.79	4.18	Up
RP14086255	Olr500	3.90	8.02	9.10	Up
RP14086989	Pramel6	3.75	4.52	5.44	Up
RP14108468	Hgf	3.15	3.74	6.07	Up
RP14108982	RGD1564345	3.18	6.32	8.11	Up
RP14130014	Slco1a2	3.20	3.40	3.96	Up
RP14131422	Plagl	3.24	3.72	4.16	Up
RP14132603	Cenc	3.17	4.21	9.26	Up
RP14169885	Naca	4.46	5.24	6.78	Up
RP14170272	Slc39a5	5.49	6.28	7.65	Up
RP14175180	Olr1084	3.14	3.22	3.42	Up
RP14175183	Olr1085	3.97	4.65	4.98	Up
RP14183524	Jrk	3.15	4.97	7.04	Up

RP14207074	Myo5a	3.37	4.16	4.77	Up
RP14211530	Traip	3.45	5.65	6.02	Up
RP14222274	Crygb	3.80	5.65	6.50	Up
RP14235002	Olr1389	3.38	3.57	5.12	Up
RP14271990	Ccz1	3.69	3.98	5.10	Up
RP14279738	Pla2g1b	3.73	4.07	4.56	Up
RP14288987	Usf1	3.09	3.16	3.85	Up
RP14301839	Inpp5j	3.49	7.37	8.39	Up
RP14329375	Ddx41	3.38	6.09	6.58	Up
RP14335189	Psm2	3.35	3.78	3.78	Up
RP14338669	Fundc2	4.84	8.01	10.45	Up
RP14344056	Dtwd2	3.03	6.60	10.47	Up
RP14344660	Slc12a2	3.32	4.88	6.02	Up
RP14359583	Olr1696	3.46	5.37	6.49	Up

2

3

Table 4(on next page)

The number of differentially expressed genes (DEGs) in three hexanal exposure group with 1.5-fold change cutoff and p-value <0.05).

The number of differentially expressed genes (DEGs) in three hexanal exposure group with 1.5-fold change cutoff and p-value < 0.05).

1 Table 4. The number of differentially expressed genes (DEGs) in three hexanal exposure group with 1.5-fold change cutoff and p-value < 0.05).

	Up-regulated genes	Down-regulated genes	Total genes
Low dose (600 ppm)	73	570	643
Middle dose (1,000 ppm)	600	211	811
High dose (1,500 ppm)	359	210	569

2

Table 5 (on next page)

GO (Gene Ontology) analysis of target genes show that the key biological processes under hexanal inhalation exposure (p-value < 0.05).

GO (Gene Ontology) analysis of target genes show that the key biological processes under hexanal inhalation exposure (p-value < 0.05).

1 Table 6. GO (Gene Ontology) analysis of target genes show that the key biological processes under hexanal inhalation exposure (p-value < 0.05).

GO Accession No.	GO Term	Count	p-value	Genes
GO:0007595	Lactation	4	0.001	NM_013197(ALAS2), NM_012630 (PRLR), NM_001012027(SERPINC1), NM_001013248(FOXB1)
GO:0035914	Skeletal muscle cell differentiation	3	0.015	NM_017259(BTG2), NM_024388(NR4A1), NM_013220(ANKRD1)
GO:0051965	Positive regulation of synapse assembly	3	0.023	NM_134376(CLSTN3), NM_001109430(LRTM2), NM_012892(ASIC2)
GO:0006814	Sodium ion transport	3	0.037	NM_001113335(SLC9A2), NM_012892(ASIC2), NM_001109385(SLC9B2)
GO:0009612	Response to mechanical stimulus	3	0.037	NM_017259(BTG2), NM_012892(ASIC2), NM_021836 (JUNB)
GO:0032680	Regulation of tumor necrosis factor production	2	0.025	NM_133290(ZFP36), NM_001106864 (LTF)
GO:0060213	Positive regulation of nuclear-transcribed mRNA poly(A) tail shortening	2	0.025	NM_133290(ZFP36), NM_017259(BTG2)

2

Table 6 (on next page)

The number of correlated target genes between DNA methylation and mRNA expression by hexanal exposure (p-value < 0.05).

The number of correlated target genes between DNA methylation and mRNA expression by hexanal exposure (p-value < 0.05).

1 Table 5. The number of correlated target genes between DNA methylation and mRNA expression by hexanal exposure (p-value < 0.05).

2

	Hyper-methylated vs. Down-regulated	Hypo-methylated vs. Up-regulated
Low dose (600 ppm)	7	0
Middle dose (1,000 ppm)	24	25
High dose (1,500 ppm)	44	28

3